Published in final edited form as:

Eur J Pharm Biopharm. 2015 September ; 95(Pt B): 239–249. doi:10.1016/j.ejpb.2015.02.013.

Intracellular delivery of dendrimer triamcinolone acetonide conjugates into microglial and human retinal pigment epithelial cells

Siva P. Kambhampati[a,b,1], **Manoj K. Mishra**[a,b,1], **Panagiotis Mastorakos**[a], **Yumin Oh**[a], **Gerard A. Lutty**[a], and **Rangaramanujam M. Kannan**[a,b,*]

[a]Center for Nanomedicine, Wilmer Eye Institute, Department of Ophthalmology, Johns Hopkins University School of Medicine, Baltimore, MD, USA

[b]Department of Biomedical Engineering, Wayne State University, Detroit, MI, USA

Abstract

Triamcinolone acetonide (TA) is a potent, intermediate-acting, steroid that has anti-inflammatory and anti-angiogenic activity. Intravitreal administration of TA has been used for diabetic macular edema, proliferative diabetic retinopathy and exudative age-related macular degeneration (AMD). However, the hydrophobicity, lack of solubility, and the side effects limit its effectiveness in the treatment of retinal diseases. In this study, we explore a PAMAM dendrimer-TA conjugate (D-TA) as a potential strategy to improve intracellular delivery and efficacy of TA to target cells. The conjugates were prepared with a high drug payload (~21%) and were readily soluble in saline. Compared to free TA, D-TA demonstrated a significantly improved toxicity profile in two important target [microglial and human retinal pigment epithelium (RPE)] cells. The D-TA was ~100-fold more effective than free TA in its anti-inflammatory activity (measured in microglia), and in suppressing VEGF production (in hypoxic RPE cells). Dendrimer-based delivery may improve the efficacy of TA towards both its key targets of inflammation and VEGF production, with significant clinical implications.

Keywords

Dendrimer; Ocular drug delivery; Triamcinolone acetonide; Anti-inflammatory; Anti-VEGF; Microglial cells; Human retinal pigment epithelium

*Corresponding author. Center for Nanomedicine, Wilmer Eye Institute, Department of Ophthalmology, Johns Hopkins University School of Medicine, 400 North Broadway, Baltimore, MD 21231, USA. Tel: +1 443 287 8634; fax: +1 443 287 8635. krangar1@jhmi.edu (R.M. Kannan).

[1]Authors with equal contribution to this work

Conflict of interest

There is no conflict of interest.

Appendix A. Supplementary material

Supplementary data associated with this article can be found, in the online version, at http://dx.doi.org/10.1016/j.ejpb.2015.02.013.

1. Introduction

Synthetic corticosteroids such as triamcinolone acetonide (TA) have both anti-inflammatory and anti-angiogenic activity, and are therefore potentially viable therapeutic options for treating various inflammatory and neovascular ocular diseases [1,2]. TA is an FDA-approved glucocorticosteroid administered intravitreally for the treatment of diabetic macular edema, macular edema associated with retinal vein occlusion [3], proliferative diabetic retinopathy [4], uveitis [5,6], sympathetic ophthalmia, and used as off-label drug for some forms of age-related macular degeneration (AMD) [7–9]. It has also been used for post-operative retinal surgery related inflammation [10]. A combination therapy of intravitreal TA (IVTA) along with photodynamic therapy (PDT) showed beneficial clinical outcomes with better visual acuity than PDT alone and reduced number PDT sessions required [11,12]. However, IVTA is often associated with side effects including elevation of intraocular pressure (IOP), cataractogenesis, photoreceptor cell death and retinal toxicity [13].

Solubilizing hydrophobic drugs such as TA is a challenge. Increasing the solubility of TA can lead to an increase in bioavailability, permeation through ocular tissue, and intracellular transport. If better drug solubility is achieved, it may result in prolonged efficacy at significantly lower concentration thereby reducing the chances of drug toxicity [14,15]. Following, intravitreal administration, TA forms epi-retinal crystals in the vitreous humor due to its lack of solubility [16], prolonging the therapeutic effect of TA, but may also cause side effects [16]. Drug aggregation and precipitation can lead to visual obscurity, unequal distribution, mechanical damage and local toxicity to the retinal tissue [16,17]. To address insolubility and sedimentation issues, TA formulations with benzyl alcohol or benzalkonium chlorides as vehicle preservatives were commercialized but resulted in vehicle-mediated toxicity and sterile-endophthalmitis [18,19].

PAMAM dendrimers are a class of well-defined, hyperbranched polymeric nanocarriers that are being investigated for ocular drug and gene delivery [20,21]. Their favorable properties such as small size, multivalency and water solubility can provide significant opportunities for many biologically unstable, hydrophobic drugs [22,23]. For example, dendrimer encapsulation of anti-glaucoma drugs resulted in better efficacy and also increased the drug uptake in corneal cell layers [15,24]. We have previously reported that, intravitreal administration of dendrimer fluocinolone acetonide (D-FA) conjugates selectively co-localized in activated microglial cells and provided sustained neuroprotection for a period of 30 days at a 40-fold lower dose compared to non-erodible controlled release implant for FA, in a rat RCS model of retinitis pigmentosa [25]. Upon systemic administration, dendrimer N-acetyl cysteine conjugates (D-NAC) targeted activated microglia in the brains of newborn rabbits with cerebral palsy, and significantly improved motor function, and reduced neurological injury [26,27]. We reported dendrimer-TA based gene delivery platform for improved delivery of genes and enhanced transfection in human retinal pigment epithelial cells [28]. Such targeting and enhanced permeation is desirable for intracellular delivery of corticosteroids to activated microglia that are located in deep layers of retina and RPE cells that have low permeability due to their tight junctions.

Despite its drawbacks, several pre-clinical and clinical studies have reported the multimodal therapeutic effects of TA [29]. For instance, TA demonstrated anti-inflammatory effect and inhibited microglial activation by suppressing the release of inflammatory cytokines and nitric oxide (NO) [30,31]. TA reduced VEGF expression in retinal pigment epithelium (RPE) cultures that were subjected to oxidative stress. Similar results were achieved in vivo with significant reduction of neovascularization in many clinically relevant animal models [10,4,32,33]. TA improves blood retinal barrier (BRB) health by enhancing the expression of adhesion molecules in endothelial cells [34,35], and significantly suppresses the blood vessel formation in choroidal endothelial cells [36]. These studies underscore the potential of TA as a drug, which can be further enhanced through superior intracellular delivery D-TA conjugates may be a viable formulation for targeted intracellular delivery of TA.

In this study, we investigate the ability of PAMAM dendrimers to deliver TA into activated microglia and human RPE cells, thus increasing its therapeutic effect. We synthesize, characterize and evaluate the efficacy of dendrimer-TA conjugates, relating to its anti-inflammatory and anti-angiogenic activity. D-TA improved the solubility of TA with reduced toxicity, improved cellular uptake and intracellular trafficking.

2. Materials and methods

2.1. Chemicals and reagents

Hydroxyl- and amine-functionalized ethylenediamine core generation four PAMAM dendrimers (G4-OH; diagnostic grade; 64 end-groups) were purchased from Dendritech Inc. (Midland, MI, USA). Triamcinolone acetonide (TA), glutaric anhydride, piperidine, *N,N'*-diisopropylethylamine (DIEA), trifluoroacetic acid (TFA), anhydrous dimethylformamide (DMF), dimethylacetamide (DMA) and 6-(Fmoc-amino) caproic acid were purchased from Sigma–Aldrich (St. Louis, MO, USA). (Benzotriazol-1-yloxy)tripyrrolidino-phosphonium hexafluorophosphate (PyBOP) was purchased from Bachem Americas Inc. (Torrance, CA, USA). Cy5-mono-NHS ester was purchased from Amersham Biosciences-GE Healthcare (Pittsburgh, PA, USA). ACS grade DMF, dichloromethane (DCM), diethylether, hexane, ethyl acetate, HPLC grade water, acetonitrile, and methanol were obtained from Fisher Scientific and used as received for dialysis, purification and column chromatography. Dialysis membrane (MW cut-off 1000 Da) was obtained from Spectrum Laboratories Inc. (Rancho Dominguez, CA, USA).

The reactions were carried out under nitrogen. Thin-layer chromatography (TLC) was performed on silica gel GF_{254} plates (Whatman, Piscataway, NJ), and the spots were visualized with UV light. Proton NMR spectra of the final conjugates as well as intermediates were recorded on a Bruker (500 MHz) spectrometer using commercially available DMSO-d_6 solvent. Proton chemical shifts were reported in ppm (δ) and tetramethylsilane (TMS) used as internal standard. All data were processed using ACD/NMR processor software (Academic Edition).

2.2. Synthesis of dendrimer conjugates

2.2.1. Synthesis of triamcinolone acetonide-21-glutarate (TA-linker, 1)—

Triamcinolone acetonide-21-glutarate (TA-Linker, 1) was synthesized using a previously established procedure [28]. A detailed synthesis description is provided as a part of supplementary information.

2.2.2. Synthesis of dendrimer-triamcinolone acetonide conjugates (D-TA, 2)—

TA-21-glutarate (TA-Linker, 139.8 mg, 0.255 mmol) was dissolved in anhydrous DMF (5 mL) in a 50 mL round bottomed flask under nitrogen, to which PyBOP (266.2 mg, 0.516 mmol) dissolved in DMF (5 mL) and DIEA(200 μL) was added, and the reaction mixture was allowed to stir for 1 h in an ice bath. PAMAM G4-OH (238.8 mg, 0.017 mmol) dissolved in anhydrous DMF (10 mL) was added drop wise to the reaction mixture above, and stirred for 48 h under nitrogen. The mixture of solvents was evaporated at 25 °C under vacuum. The crude product was redissolved in DMF (20 mL) and subjected to dialysis in DMF (membrane MW cutoff = 1 kDa) for 24 h, where the solvent was changed at least 4 times. The obtained solution was evaporated under reduced pressure at room temperature, followed by high vacuum overnight, to produce an off-white semi-solid dendrimer-triamcinolone conjugate (D-TA, 470.9 mg). The resultant semi solid product was dissolved in ice cold DI water and dialyzed against DI water (membrane MWCO = 1 kDa) at 4 °C for 5 h by changing the water every hour to remove traces of DMF. The resultant water layer was lyophilized to get fluffy white powder of D-TA (402.3 mg) (Fig. S1–B). The D-TA conjugates were characterized by ^{1}H NMR for drug loading and reverse-phase HPLC for purity. ^{1}H NMR (DMSO-d_6) d 0.82 (s, −CH_3 protons of TA), 1.14 (s, −CH_3 protons of TA), 1.34 (s, −CH_3 protons of TA), 1.49 (s, −CH_3 protons of TA), 1.53–2.05 (m, −CH protons of TA, − CH_2 protons of linker), 2.20 (brs, −CH_2 protons of G4-OH), 2.31–2.48 (m, −CH protons of TA, −CH_2 protons of linker, −CH_2 protons of G4-OH), 2.64 (bs, −CH_2 protons of G4-OH), 3.09–3.11 (t, −CH_2 protons of G4-OH), 3.28 (m, −CH_2 protons of G4-OH), 3.38–3.40 (t, −CH_2 protons of G4-OH), 3.58 (s, −CH protons of TA), 4.00–4.02 (m, CH_2OC= O protons, G4-OH), 4.20 (brs, −CH protons of TA), 4.73–6.01 (singlets and doublets, −CH protons of TA, OH protons of G4-OH), 6.22–7.31 (two doublets, aromatic protons of TA), 7.79–8.07 (m, amide protons of G4-OH).

2.2.3. Synthesis of intermediate dendrimer conjugates—

The synthesis protocols for the intermediate conjugates D-OH-NHFmoc (**3**), Fmoc-functionalized intermediate D-TA (**4**) and NH_2-D-TA (**5**) are provided as part of supplementary information.

2.2.4. Synthesis of Cy5-labeled dendrimer-triamcinolone acetonide conjugates (Cy5-D-TA, 6)—

The NH_2-D-TA (**5**), (25 mg, 0.0013 mmol) was dissolved in 1 mL of borate buffer (pH 9.0) at room temperature. The reaction mixture was cooled to 0 °C, and Cy5 mono NHS ester (2.18 mg, 0.0027 mmol) dissolved in 1 ml of DMF was added. *N*-Hydroxysuccinimide (1.58 mg, 0.013 mmol) dissolved in 500 μL of DMF was added to reaction. The reaction mixture was stirred overnight at room temperature. The crude product was dissolved in water and subjected to dialysis against pure DI water (membrane MWCO = 1 kDa) for 12 h with successive change of water in every 2 h at 4 °C. The resultant water layer was lyophilized to get Cy5-D-TA, 5 (12.8 mg). The Cy5-D-TA was characterized by

reverse-phase HPLC for purity, and fluorescence spectroscopy. ^{1}H NMR (DMSO-d_6) δ 0.82 (s, −CH_3 protons of TA), 1.14 (s, −CH_3 protons of TA), 1.23–1.26 (m, −CH_2 protons of linker), 1.34 (s, −CH_3 protons of TA), 1.48–1.52 (s, −CH_3 protons of TA, −CH_2 protons of linker), 1.69–2.04 (m, −CH protons of TA, −CH_2 protons of linker), 2.20 (bs, −CH_2 protons of G4-OH), 2.39–2.47 (m, −CH protons of TA, −CH_2 protons of linker and −CH_2 protons of G4-OH), 2.64 (bs, −CH_2 protons of G4-OH), 3.09–3.11 (t, −CH_2 protons of G4-OH), 3.38–3.40 (t, −CH_2 protons of G4-OH), 4.00–4.01 (d, CH_2OC= O protons of G4-OH), 4.20–7.33 (singlet and doublet, −CH and aromatic protons of TA and Cy5), 7.65 (s, aromatic protons of Cy5), 7.79–8.05 (m, amide protons of G4-OH), 8.38 (m, aromatic protons of Cy5).

2.3. Characterization of the conjugates

2.3.1. High performance liquid chromatography (HPLC)—The purity of the dendrimer conjugates was analyzed by HPLC (Waters Corporation, Milford, MA) equipped with a 1525 binary pump, a 2998 photodiode array (PDA) detector, a 2475 multi-wavelength fluorescence detector, and a 717 auto sampler (kept at 4 °C) interfaced with Empower software. The HPLC chromatograms were monitored at 205 (G4-OH) and 238 nm (TA conjugated dendrimers) using PDA detector. For Cy5-labeled conjugates, fluorescence detector was used for the detection (excitation: 645 nm and emission: 662 nm). The water/acetonitrile (0.1% w/w TFA) was freshly prepared, filtered, degassed, and used as mobile phase. A TSK gel ODS-80 Ts (250 × 4.6 mm, i.d., 5 μm) with TSK gel guard column were used for the study (Tosoh Bioscience LLC, Japan). A gradient flow was used with initial condition of 90:10 (H_2O/ACN) was maintained until 20 min and gradually changing the ratios to 10:90 (H_2O/ACN) at 40 min and returning to initial conditions 90:10 (H_2O/ACN) in 60 min with flow rate of 1 mL/min for all conjugates.

2.3.2. Dynamic light scattering (DLS) and zeta potential (ζ)—The particle size and ζ-potential of G4-OH, and their respective conjugates were determined by dynamic light scattering (DLS) using a Zetasizer Nano ZS (Malvern Instrument Ltd. Worchester, UK) equipped with a 50 mW He—Ne laser (633 nm). The conjugates (G4-OH, D-TA and NH_2-D-TA) were dissolved in deionized water (18.2 Ω) to make the solution with the final concentration of 0.1 mg/mL The solution was filtered through a cellulose acetate membrane (0.45 μm, PALL Life Science) and DLS measurements were performed in triplicate, at 25 °C with a scattering angle of 173°.

2.3.3. Drug release study in simulated vitreous humor—The release of TA from the D-TA conjugate was characterized in simulated vitreous humor [Hanks balanced salt solution with 0.03% sodium hyaluronate (Lifecore biomedical, MN, USA) and 0.1% Tween 80 (DakoCytomation, CA, USA)] as a stabilizer and surfactant to reduce released TA settling. A concentration of 3 mg/mL was maintained in water bath at 37 °C equipped with shaker. At appropriate time points, 200 μL of solution was withdrawn from the incubation mixture, frozen in liquid nitrogen and lyophilized. To this lyophilized powder, 400 μL of 50:50 (DCM:EtOAc) was added and sonicated for 10 min and centrifuged at 10,000 rpm for 5 min at 4 °C. The supernatant was collected and the solvent was evaporated by nitrogen flush and reconstituted with 200 μL of 50:50 H_2O:ACN and subjected to HPLC analysis

following the method described in HPLC section. The percent of released TA from D-TA was quantified using the calibration graph.

2.4. In-vitro characterization of the conjugates

2.4.1. Cell culture—Murine brain microglial cells (BV-2) passage 18 (P:18) were cultured in Dulbecco's modified Eagle's medium (DMEM, Life technologies, Grand Island, NY) supplemented with 5% heat in activated fetal bovine serum (Hi-FBS, Invitrogen Corp., Carlsbad, CA) and 1% antibiotics (penicillin/streptomycin) (Invitrogen Corp., Carlsbad, CA). Human retinal pigment epithelial cells (ARPE-19) passage 21 (P: 21) were cultured in DMEM/F12(1:1) (Life technologies, Grand island, NY) supplemented with 10% HI-FBS and 1% antibiotics. The above mentioned cell cultures were in a humidified incubator at 37 °C with 5% CO_2.

2.4.2. Cytotoxicity assay—BV-2 and ARPE-19 cells were plated at a concentration of 1.0×10^4/well in a 96 well plate (Costar, Cambridge, MA) and incubated at 37 °C for 24 h in their respective growth medium. After 24 h the cells were treated with medium containing different concentrations (0.1–200 μg) of TA and D-TA at increasing concentrations for 24 h. The cells treated with fresh medium serves as control. Cell viability was assessed using MTT cell proliferation assay kit (Molecular probes, Invitrogen, Oregon, USA). Absorbance was read at 540 nm using fluorescence microplate reader (BioTek Instruments, Winooski, Vermont, USA) and cell viability was determined as percent absorbance relative to untreated control cells.

2.4.3. Anti-inflammatory assay in microglial cells—Microglial (BV-2) cells were plated at a concentration of 1×10^6 cells per well in a 12 well plate. After 24 h the microglial cells were activated using Lipopolysaccharides (LPS) (Sigma, St Louis, MO) at a concentration of 100 ng/mL for 3 h. After 3 h of pre-activation of microglial cells the activated microglial cells confirmed as they assume an amoeboid shape, the cells were treated with 1 mL of medium with 100 ng of LPS containing various concentrations of free TA (1–100 μg) and D-TA containing equivalent concentration conjugated TA that of free TA treated for 12 h. A stock solution of 10 mg/mL of free TA was prepared by dissolving TA in absolute ethanol and subjected to serial dilution immediately to obtain desired concentration thereby avoid settling of TA particles in aqueous medium. Whereas D-TA being water soluble was dissolved in medium and serially diluted to obtain desired concentrations. After 12 h the medium containing free TA and D-TA was removed and the cells were washed with warm medium and replenished with new medium containing LPS.

The cell culture medium was sampled at 24 h and 48 h, immediately centrifuged at 1500 rpm for 5 min at 4 °C and subjected for TNF-α cytokine levels using a mouse TNF-α ELISA kit (R&D systems, Minneapolis, MN, USA).

2.4.4. Anti-VEGF activity in oxidative stress exposed retinal pigment epithelial cells—Retinal pigment epithelial cells (ARPE-19) cells were plated at an initial concentration of 1×10^6 cells per well in a 12 well plate. After 24 h the medium was changed every day until day 5 to form RPE monolayers. The monolayers were exposed to

hypoxia in a low oxygen incubator in a humidified atmosphere for 8 h and medium is rapidly changed to fresh medium and incubated normal culture conditions (reoxygenation) for 2 h. After reoxygenation the monolayers were exposed to various concentrations of free TA and D-TA containing equivalent concentrations of TA in conjugated form for 24 h. The monolayers with no treatment serves as positive control and the monolayers which were not exposed to hypoxia serve a negative control. After 24 h of treatment the treatment medium was removed and the monolayer was washed with warm medium twice to remove any TA or D-TA particles and replaced with fresh medium and incubated at 37 °C overnight (18 h). The culture medium was collected in 2 mL vials and centrifuged at 1000 rpm for 5 min at 4 °C to remove debris, the supernatant was immediately assessed for VEGF levels were assessed using human VEGF ELISA kit (R&D systems, Minneapolis, MN, USA). Optical density at the end point was measured at 540 nm with wavelength correction at 570 nm using fluorescence microplate reader (BioTek Instruments, Winooski, Vermont, USA). The VEGF levels were calculated using the calibration graph according to the manufacturer's instructions.

The monolayers were subjected to trypsin treatment and the cell pellets were collected via centrifugation. Total RNA was purified with TRIzol reagent (Life Technologies, Grand Island, NY) following the manufacturer's instruction. 3 μg of total RNA was reverse-transcribed to cDNA using High-capacity cDNA Reverse Transcription System (Life Technologies) according to the manufacturer's instructions. qRT-PCR was performed with fastSYBR Green Master Mix (Life Technologies) by a StepOnePlus Real-Time PCR System (Life Technologies). The sequence of primer used for human VEGF forward primer 5'-CAGCGCAGCTACTGCC ATCCAATCGAGA-3', and reverse primer, 5'-GCTTGTCACATCTG CAAGTACGTTCGTTTA-3' was used for amplification. Human GAPDH forward 5'-AATCCCATCACCATCTTCCA-3', reverse 5'-TG GACTCCACGACGTACTCA-3' was used to normalize the expression levels of target gene and calculated by the comparative cycle threshold Ct method ($2 - \Delta\Delta Ct$).

2.5. Cell uptake and intracellular localization of D-TA

2.5.1. Flow cytometry—The cellular uptake of Cy5-D-TA was measured via flow cytometric analysis. Cells were seeded in 12-well plates at an initial concentration of 1.0×10^5 cells/well and left to attach overnight. Cells were incubated with Cy5-D-TA or D-Cy5 at 2 μ.g/ml (on equivalent fluorescence of Cy5 both in Cy5-D-TA and D-Cy5); at different time points (1, 3, 6 and 12 h) the media was removed and cells were washed with 1 × PBS as well as Trypan blue prior to being incubated with 1 volume of 0.25% Trypsin with EDTA for 5 min at 37 °C. Two volumes of DMEM medium with 10% FBS were added to neutralize trypsin. The cellular uptake of D-TA was measured using the Accuri C6 flow cytometer (BD Biosciences, San Jose, CA) with an FL4 band-pass filter with emission detection wavelength of 675/25 nm. Data were analyzed using the BD Accuri C6 software. The thresholds were set using untreated samples.

2.5.2. Confocal microscopy—ARPE-19 cells were seeded at a concentration of 1×10^5 in a glass 35 mm glass bottom culture dish (MatTek Corporation, Ashland, MA). The cells were incubated with Cy5-D-TA or D-Cy5 as a control at 2 μg/mL and at different time

points (1 h, 3 h, 6 h and 12 h) the media were removed and cells were washed with 1 × PBS twice and fixed with 4% PFA and blocked with normal goat serum (NGS) for 2 h at 4 °C. The blocked cells were stained for glucocorticoid receptors (GR) using anti-GR antibody (abcam) (1:200) overnight at 4 °C and then goat α rabbit Cy3 conjugated secondary antibody (life technologies) (1:100) for 4 h. The cells were washed and stained with DAPI (1:1000) for 10 min and imaged using confocal Zeiss LSM 710 microscope.

3. Results and discussion

3.1. Preparation of dendrimer-TA conjugate (D-TA, 2)

The ester-linked dendrimer-triamcinolone acetonide (D-TA, ***2***) was prepared by a two-step process as shown in Fig. 1, and characterized by ^{1}H NMR and HPLC. TA was functionalized with a carboxylic acid terminal group using glutaric acid as spacer. In brief, TA was reacted with glutaric anhydride dissolved in DMA/DMF mixture in the presence of a base to get the TA-linker (***1***). The most reactive hydroxyl group at 21-position was reacted with anhydride to get an ester linkage. The structure of TA-linker was established by ^{1}H NMR and the purity was determined by HPLC. In ^{1}H NMR, characteristic peaks at 1.79,2.32 and 2.47 ppm for CH_2 protons of the linker, and a peak at 12.12 ppm corresponding to carboxylic acid confirmed the formation of the TA-linker. The TA-linker was further conjugated with PAMAM dendrimer (G4-OH) using PyBOP as coupling reagent to get therapeutic conjugate, D-TA (***2***). In ^{1}H NMR spectrum, four peaks in between 0.82 and 1.49 ppm represent methyl protons of the TA. Additionally, as shown in Fig. 2A, apart from dendrimer and TA peaks in between 2.0 and 8.1 ppm, a characteristic peak at 4.01 ppm was observed which corresponds to methylene protons of the dendrimer reacted with TA. Using NMR proton integration technique, we estimated that approximately 10 molecules of TA were conjugated to one dendrimer molecule (~21%). The conjugate is readily soluble in DI water, PBS buffer and saline, in contrast to free TA which has poor water solubility (Fig. S4). The maximum solubility of free TA reported to be 21 μg/mL in PBS [37], whereas achieved-TA is soluble up to 4 mg/mL (on a TA basis), and corresponds to a 200-fold enhancement in solubility.

The purity of the conjugate and the TA-linker were determined using reverse phase HPLC. The hydrophobic free TA eluted at 37.1 min, whereas the TA-linker eluted at 39.0 min (with no trace at 37.1 min). At similar HPLC conditions, a broad peak at 36.0 min was observed for D-TA conjugate (monitored at 238 nm) which is different from that for the starting dendrimer (retention time 15 min). The conjugate is largely pure since we did not observe any ‘characteristic’ peaks related to free TA and TA-linker. The broad peak of D-TA conjugate can be attributed to the high loading of TA (~10 molecules per dendrimer) resulting in some non-polar character.

3.2. Preparation of Cy5 labeled dendrimer-triamcinolone acetonide conjugate (Cy5-D-TA, 6)

The Cy5-D-TA conjugate was prepared using a four-step process following a modified synthetic procedure published recently [28], (Fig. 1). In the publication mentioned above, we have reported the preparation of Cy5-D-TA conjugate with more than 20 surface amine groups for the gene delivery study. For the present study, we designed Cy5-D-TA (***6***) with

fewer amine groups on the surface of the conjugate, so that we could reacts approximately one molecule of Cy5. In brief, Fmoc-caproic acid was reacted with the dendrimer using PyBOP as coupling agent, to get Fmoc-functionalized dendrimer (D-OH-NHFmoc, ***3***). Three multiplets (1.24–1.51 ppm) for caproic acid CH_2 protons, a singlet at 4.00 ppm for internal CH_2 protons of G4-OH, and multiplets between 7.26 and 7.68 ppm for Fmoc aromatic protons in NMR spectra confirmed the formation of the intermediate (Fig. S3). Using proton integration method, it was estimated that 7 linker molecules were reacted with the dendrimer. Further, the Fmoc-functionalized dendrimer (***3***) was reacted with TA-linker using PyBOP/DIEA to get Fmoc functionalized D-TA (***4***). In the ^{1}H NMR spectrum, peaks at 0.84–1.50 ppm represent methyl protons of TA, and peaks at 4.75–6.25 ppm represent aromatic protons of TA along with dendrimer peaks confirmed the formation of the conjugate. The Fmoc groups were deprotected with piperidine in DMF to get dendrimer-TA conjugate (NH_2-D-TA, ***5***) and characterized by ^{1}H NMR. The NH_2-D-TA conjugate has few free amine groups which would react with Cy5. In the NMR spectrum, absence of aromatic Fmoc protons signal and presence of all signals related to TA confirmed the formation of the product. As per proton integration analysis, 6 molecules of TA and ~3 amine groups were present in NH_2-D-TA conjugate (Fig. S4). Finally, Cy5-mono-NHS ester was reacted with NH_2-D-TA in DMSO/buffer (pH 8.9) mixture to get Cy5-labeled den-drimers-TA conjugate, Cy5-D-TA (***6***). The final conjugate was purified by dialysis and further by GPC fractionation and characterized by reverse-phase HPLC and NMR spectroscopy. In NMR spectrum, peaks corresponding to TA and linker molecules were present as mentioned above along with Cy5 peaks (Fig. 2B). In HPLC analysis free Cy5 eluted at 15.05 min whereas Cy5-D-TA eluted at 33.08 min as a broad peak (monitored at 645 nm excitation) confirming the formation of the conjugate free from unreacted dye. Since one molecule of Cy5 dye was used in the reaction, we could not see intense peak in the NMR spectrum in aromatic region.

3.2.1. Particle size and zeta potential—Size and surface charge of the dendrimer conjugate influences its cellular entry, receptor binding or targeting to specific site of the tissue [22,38]. We investigated the particle size and zeta potential G-OH (D), D-TA, and NH_2-D-TA. The size of G4-OH was 4.4 ± 0.2 nm and zeta potential was slightly positive (4.5 ± 0.2 mV) due to their tertiary amines in its core. Upon conjugating ~10 molecules of TA to the dendrimer there was small increase in size (5.2 ± 0.3 nm), but there was no change in its surface charge (4.2 ± 0.7 mV). In the case of NH_2-D-TA conjugate the size and zeta potential were 5.0 ± 0.5 nm and 5.9 ± 0.2 mV respectively. There is a small increase in the zeta potential due to the presence of 3–4 primary amine groups on the dendrimer surface after deprotection, which was further used for Cy5 conjugation. We could not analyze the size and zeta potential of Cy5-D-TA due to the presence of Cy5 molecule and its interference with the laser used in the zetasizer.

3.2.2. Release study—*In vitro* release characteristics of D-TA conjugate were investigated in simulated vitreous humor as a physiologically relevant pH 7.0 mimicking the intravitreal injection of D-TA conjugates. A calibration curve for both TA and TA-linker was established over a concentration of 10 ng to 20 μg at 238 nm. We used HPLC method to quantify the release characteristics of the D-TA conjugate. The conjugate has two ester linkages that are susceptible to hydrolysis (i) an ester linkage between the −OH group of the

dendrimer surface and the −COOH group of the TA-linker and (ii) another ester linkage between the hydroxyl group at 21-position of TA and the carboxyl group (−COOH) of one end of the glutaric acid linker. Our results suggest that the drug was released as free TA and TA-linker, confirmed by the two peaks that appeared in the HPLC chromatogram that coincide with the retention time of TA and TA-linker. Since there was an overlap of the peaks between the released drug forms and the conjugates, we adopted solvent precipitation method for extracting the released TA and TA-linker from the incubation mixture. The conjugates were insoluble in organic phase (DCM/ethyl acetate, 50:50) and precipitated out, while the organic phase containing the drug and drug linker was reconstituted in HPLC mobile phase and analyzed.

D-TA conjugates released the drug more in the form of TA-linker than as TA. This phenomenon was also reported by Macky et al. [31] where the ester bond between the TA and the linker was more stable for a period of 7 days. The conjugates exhibited initial burst release of ~18% of its payload within 24 h. From day 3 to day 20, there was a sustained release, with a further ~40% release, followed by a nearly zero order release over the period from day 20 to day 45, resulting in ~95% of the payload released (Fig. 3C). The hydroxyl group in TA used in the conjugation is not required for any therapeutic activity or receptor binding [39,40] and thus the dendrimer-TA may be able to maintain the same therapeutic activity as that of free TA.

3.3. Efficacy of D-TA conjugates in microglial and RPE cells

3.3.1. D-TA conjugates were less cytotoxic than free drug—The D-TA conjugates should be non-cytotoxic at the concentrations used in cell studies. We performed a cell viability assay to establish the range of concentrations where both free TA and D-TA are non-toxic, to establish the therapeutic window for efficacy studies in cells. Previous studies showed that 400 μg/mL TA was toxic to retinal cells largely due to drug precipitation and crystal formation [16], hence we treated the cells with preservative free TA within the concentration range from 0.1 to 200 μg/mL of TA and D-TA which contains equivalent concentrations of TA. We also tested the toxicity of free dendrimer based on the amount of den-drimer present in D-TA. Since we used ethanol to dissolve free TA and serially diluted with cell medium we also used the same amount of ethanol for D-TA and controls. The ethanol treatment did not illicit any toxicity in both BV-2 and ARPE-19 cells. At 200 lg/mL, free TA showed significant decrease in % cell viability in BV-2 and ARPE-19 cells (58.3% ± 5.9% and 54.2% ± 6.8% respectively), but interestingly D-TA conjugates did not induce any cell death resulting (90.7% ± 8.5% and 91.6% ± 2.6%) respectively at this concentration (Fig. S5A and S5B). We noticed that at the highest concentrations (200 μg/mL) free TA precipitated and formed crystals to some extent, and deposited over the cells (Fig. S6), whereas D-TA is highly soluble and did not precipitate. Cytotoxicity of free TA can be attributed to the direct contact of the crystal formations with the cellular membrane resulting in drastic alteration in the cellular morphology and induction of the apoptotic cascade as noticed by Szurman et al. in ARPE-19 cells [41]. Similar effect was also noticed at 100 μg/mL of free TA but not with D-TA. At concentrations below 100 μg/mL, both free TA and D-TA did not show significant decrease in cell viability upon 24 h of incubation. Free

dendrimer did not show any cytotoxic effects in both cell types in any concentrations thereby negating the effect of delivery vehicle on cytotoxicity.

3.3.2. D-TA conjugates show enhanced anti-inflammatory activity in microglial cells compared to free TA—For investigating the anti-inflammatory effect of D-TA conjugates, we used LPS induced pro-inflammatory murine BV-2 microglial cells, which play a critical role in mediating retinal inflammation. LPS activates protein kinases in microglial cells through toll-like receptors (TLR) pathway thereby stimulating the release of immune regulated proinflammatory cytokines such as TNF-α, IL-1β and IL-6 [42,43]. We used TNF-α suppression to evaluate the anti-inflammatory properties of TA and D-TA. Upon LPS pretreatment, there was a significant increase (~15-fold) in TNF-α level at 24 h. We tested varying concentrations of LPS and verified that 100 μg/mL treatments did not induce any cell death at least until 72 h after incubation (data not shown). Cells were treated with free-TA or D-TA for a 12 h period, in the presence of LPS. The supernatant was replaced after 12 h, with just LPS, but no D-TA and free TA. Therefore, these studies reflect the efficacy of free TA and D-TA treatment and their uptake by the cells over a limited time of 12 h, studied at 24, 48 and 72 h, in the continuous presence of LPS over 72 h. Free TA inhibited TNF-α production in a dose dependent manner, with a maximum reduction of ~28.2% at highest treatment dose of 100 μg/mL at 24 h post treatment, whereas at low concentrations (25, 10 and 1 μg/mL) did not show any significant inhibition in TNF-α levels. In comparison, D-TA conjugate treatment, containing equivalent TA concentration (e.g. 100 μg/ mL), significantly reduced the TNF- α level (~66.4%) and exhibited superior anti-inflammatory properties compared that of free TA. At 24 h, the extent of TNF-α suppression achieved with 1 μg/mL of D-TA was better than that achieved with 100 μg/mL of free-TA. This may be attributable to the fact that the dendrimer increased the intracellular uptake of conjugated TA compared to free TA (Fig. 4A).

At 48 h post treatment, with continuous LPS exposure, free TA did not inhibit TNF-α production, even at the highest concentration (100 μg/mL). In contrast, D-TA showed significant efficacy in suppressing TNF-α production in a dose dependent manner, resulting in ~35% suppression at 1 μg/mL to ~65% at 100 μg/mL (Fig. 4B). The dose-response upon D-TA treatment and the extent of suppression was similar to that seen at 24 h, indicating that D-TA sustained the effect at least up to 48 h. At 72 h, free TA did not show any TNF-α suppression, whereas D-TA showed moderate suppression (~35% at 100 μg/mL) (Fig. 4C). The sustained anti-inflammatory effect provided by D-TA at very low concentration promises improved therapeutic effect for inflammatory retinal diseases.

3.3.3. D-TA inhibits VEGF production in hypoxic RPE cells—To examine the effects of free TA and D-TA on VEGF production, we assessed the protein and mRNA expression by ARPE-19 cells after hypoxia. We used hypoxia-reoxygenation in order to induce oxidative stress, resulting in the up regulation and secretion of VEGF in RPE, which is one of the most important causes of retinal neovascular diseases [10]. Upon 6 h of hypoxia exposure to ARPE-19 cell monolayers, we saw increased VEGF levels (2107.9 ± 230.7 pg/mL). After exposure to hypoxia followed by 2 h of re-oxygenation with fresh medium, the cells were treated with different concentrations of free TA and D-TA for 24 h and then

replaced with medium without TA or D-TA, and the VEGF ELISA was performed 24 h after medium change. Both TA and D-TA treatments inhibited VEGF secretion in a dose dependent manner. Free TA treatment led to a maximum reduction of ~27% at 100 μg/mL concentration. D-TA treatment resulted in a significantly better inhibition of VEGF secretion (~60%) at 100 μg/mL (Fig. 5A). D-TA inhibition of VEGF at 1 μg/mL was significantly better than that achieved at a 100-fold higher level of free TA.

For VEGF to be secreted from RPE, mRNA corresponding to VEGF has to be synthesized using transcription from DNA in the nucleus, from where they are released into the cytoplasm translated to VEGF protein, and further secreted from cells. Corticosteroids induce their effect via glucocorticoid receptor activation [2,3] and suppressing the mRNA levels in the nucleus. To see whether a reduced level of VEGF protein secreted by RPE cells after D-TA treatment is due to down regulation of mRNA synthesis in these cells, we performed RT-PCR analysis of mRNA isolated from the treated cells. The RT-PCR results were consistent with ELISA analysis showing VEGF protein suppression. The VEGF inhibition at the mRNA level, where 75% inhibition could be achieved with D-TA at 10–25 μg/mL, was significantly better than that for free TA (Fig. 5B). At 100 μg/mL of D-TA, the inhibition was less than that achieved at 10 or 25 μg/mL. This suggests that D-TA at too high a concentration may actually decrease efficacy, as seen in steroids in animal models of retinal diseases [44].

3.4. Cell entry and intracellular localization of D-TA conjugates

3.4.1. Enhanced cellular uptake of D-TA conjugates—Flow cytometry analysis was performed to assess the effect of TA conjugation on the cellular uptake of D-TA. Despite their similarity in size and surface properties, Cy5-D-TA demonstrated consistently higher uptake in ARPE cells in comparison with D-Cy5. Specifically, at 1, 3, 6 and 12 h the percentage of the cell population that had taken up Cy5-D-TA was 1.7-, 3.7-, 3.3- and 2.2-fold higher than that of the cells that had taken up D-Cy5, respectively. The mean fluorescence intensity demonstrated a similar correlation. As expected, the cell uptake increased over time for both D-Cy5 and Cy5-D-TA treated cells (Fig. 6). D-Cy5 was used as a control to exactly establish how the TA conjugation affects the uptake of dendrimers by the cells.

Cellular uptake constitutes an important barrier to effective delivery of anti-inflammatory therapeutics. While delivery of TA with the use of various nanocarriers has been studied, this is the first study to demonstrate that TA conjugation on the surface of dendrimers enhances cellular uptake of the conjugate. These results are in accordance with our previous work demonstrating that dendrimer-based gene vector uptake and transfection can be significantly improved following conjugation of TA [28]. This phenomenon may be attributed to TA (as a hydrophobic moiety) when conjugated to the surface of the dendrimer may improve the cell membrane–dendrimer interaction, enhance uptake and further to the nuclear localization of D-TA gene vectors leading to decreased exocytosis [45].

3.4.2. D-TA conjugates translocate to the nucleus via glucocorticoid receptors —Corticosteroids exert their anti-inflammatory and anti-VEGF activity via glucocorticoid

receptor (GR) pathway [3,46]. Many studies have previously reported that TA binds to GR, resulting in the activation of GR, followed by translocation to the nucleus [40]. In order to examine the ability of D-TA to interact with the GR and translocate to the nucleus we treated RPE cells with Cy5-D-TA and D-Cy5 and visualized intracellular trafficking using high resolution confocal microscopy at different time points. Anti-GR antibody (Cy3, green) and DAPI (blue) were used to stain the GR and nuclei respectively. In the untreated (Fig. 7A – D) and free TA treated cells (not shown), the GR receptors were seen distributed in the cytoplasm. In contrast, at 3 h, in the Cy5-D-TA treated cells, the GR were seen concentrated around the nucleus (Fig. 7E – H) (indicated by white arrows) and were further co-localized with the Cy5 signal (red, Fig. 7G) suggesting that D-TA binds to GR. Twelve hours post incubation, Cy5-D-TA and GR were co-localized in the nucleus and was confirmed by the yellow signal in merged panel (Fig. 7K – N). To depict the co-localization of Cy5-D-TA and GR, we digitally magnified a single cell at 3 and 12 h (Fig. 7I and O), indicating the GR concentrating around the nucleus and nuclear delivery of Cy5-D-TA respectively (white arrows).

The imaging results are in agreement with the flow cytometry results, indicating enhanced cellular uptake and nuclear localization of D-TA conjugates. The difference in the GR localization of the free TA and D-TA, and the fact that D-TA localizes with GR even at 3 h [when we do not expect appreciable drug release (Fig. 3C)] suggest that the dendrimer conjugate is binding to the receptor. Moreover, these results also suggest that conjugating TA to dendrimer using OH group at 21st position did not alter the binding of TA to the GR. The increased intracellular uptake of D-TA, enabled in part by TA, is in good agreement with our previous reports that D-TA based dendrimer gene carriers showed enhanced transfection in RPE cells, compared to dendrimer gene carriers [28].

4. Conclusions

Neuroinflammation and neovascularization are the two important pathological events implicated in AMD, diabetic retinopathy, CNV and other retinal diseases [47–49]. Therapies that can target both these events will be highly beneficial. Corticosteroids, particularly TA, has both anti-inflammatory and anti-angiogenic activity and has been used clinically. Improved intracellular delivery can enhance efficacy of TA and reduce its side effects [3]. In this study we synthesized hydroxyl PAMAM dendrimer based D-TA conjugate with a high payload (~21%) that were (a) highly water soluble and exhibited sustained release of TA ~2% per day for a period for ~45 days, (b) less toxic and enhanced cellular uptake of TA and (c) significantly more efficacious in its anti-inflammatory (activated microglial cells) and anti-VEGF activity (retinal pigment epithelial cells) compared to free TA.

Microglial cells perform dynamic immune surveillance and are responsible in maintaining the normal retinal health [50]. However, under pathological conditions they become activated and contribute to BRB breakdown, cytokine production and stimulating RPE to produce VEGF leading to neovascularization [3,48]. On the other hand, RPE cells are the major contributor for VEGF production [51], a factor involved in enhanced blood vessel permeability, abnormal neo-vessel formation resulting in leaky blood vessels [2]. The ability of D-TA to significantly suppress TNF-a in microglia for a period of 72 h, after a 12-h

treatment, suggests sustained anti-inflammatory action. In RPE cells, D-TA was more efficacious in inhibiting VEGF secretion, compared to a 100-fold higher concentration of free TA. In order for TA to exert its therapeutic effect, it needs to be transported into the cell, and further to the nucleus. From flow cytometry results it is evident that conjugating TA to the dendrimer enables more drug to be transported into the cells. Interestingly, presence of TA on the dendrimer seemed to increase dendrimer uptake. TA exerts its biological activity *via* glucocorticoid receptor (GR) pathway [52,53]. *In-vitro* cell experiments, flow cytometry and qualitative results from con-focal microscopy suggest that D-TA enters nucleus along with GR to express its activity. Glucocorticoids down regulate VEGF by blocking up-stream of its transcription in the nucleus [3,8,54] which is evident from confocal images and RT-PCR studies where D-TA treatment showed low levels of VEGF mRNA.

Increased efficacy and decreased toxicity achieved with dendrimer conjugation of TA may be attributed to the difference between the mechanism by which TA exert its therapeutic or cytotoxic effect. While the dendrimer conjugate properties result in improved therapeutic effect, at the same time the dendrimer prevents formation of TA crystals thus reducing TA toxicity this favorable balance may have important clinical implications. TA is typically injected in relatively large doses (4 mg in human eyes) l resulting in various side-effects such as elevated IOP, retinal toxicity and blurred vision [55]. In this study we have demonstrated that both anti-inflammatory and anti-VEGF properties of TA can be enhanced by conjugating them to dendrimers resulting in efficacy at much lower concentrations (~100 fold) than that of free drug. Therefore, dendrimer-TA conjugates may be a viable formulation for targeted intracellular delivery of TA. Further evaluation of the D-TA conjugates in clinically relevant animal models can provide more insights in terms of sustained efficacy, potentially offering a potent option for fighting against numerous retinal diseases such as AMD, CNV, diabetic retinopathy and macular edema.

Supplementary Material

Refer to Web version on PubMed Central for supplementary material.

Acknowledgments

This study was supported by funds from Wilmer Pooled Professor grant, NIH NIBIB RO1EB018306-01-(RMK) and Research to prevent blindness (RPB). We also acknowledge Wilmer core facility and imaging center (core grant: P30EY001765) for flow cytometry and confocal microscopy facilities.

References

1. Kiernan DF, Mieler WF. The use of intraocular corticosteroids. Expert Opin. Pharmacother. 2009; 10:2511–2525. [PubMed: 19761356]
2. Ayalasomayajula SP, Ashton P, Kompella UB. Fluocinolone inhibits VEGF expression via glucocorticoid receptor in human retinal pigment epithelial (ARPE-19) cells and TNF-a-induced angiogenesis in chick chorioallantoic membrane (CAM). J. Ocul. Pharmacol. Ther. 2009; 25:97–104. [PubMed: 19284324]
3. Zhang X, Wang N, Schachat AP, Bao S, Gillies MC. Glucocorticoids: structure, signaling and molecular mechanisms in the treatment of diabetic retinopathy and diabetic macular edema. Curr. Mol. Med. 2014; 14:376–384. [PubMed: 24467200]

4. Zhang X, Bao S, Lai D, Rapkins RW, Gillies MC. Intravitreal triamcinolone acetonide inhibits breakdown of the blood-retinal barrier through differential regulation of VEGF-A and its receptors in early diabetic rat retinas. Diabetes. 2008; 57:1026–1033. [PubMed: 18174522]
5. Salek SS, Leder HA, Butler NJ, Gan TJ, Dunn JP, Thorne JE. Periocular triamcinolone acetonide injections for control of intraocular inflammation associated with uveitis. Ocul. Immunol. Inflamm. 2013; 21:257–263. [PubMed: 23617776]
6. Li W, He B, Dai W, Zhang Q, Liu Y. Evaluations of therapeutic efficacy of intravitreal injected polylactic-glycolic acid microspheres loaded with triamcinolone acetonide on a rabbit model of uveitis. Int. Ophthalmol. 2014; 34:465–476. [PubMed: 23868505]
7. Becerra ME, Morescalchi F, Gandolfo F, Danzi P, Nascimbeni G, Arcidiacono B, et al. Clinical evidence of intravitreal triamcinolone acetonide in the management of age-related macular degeneration. Curr. Drug Targets. 2011; 12:149–172. [PubMed: 20887246]
8. Penfold PL, Wong JG, Gyory J, Billson FA. Effects of triamcinolone acetonide on microglial morphology and quantitative expression of MHC-II in exudative age-related macular degeneration. Clin. Exp. Ophthalmol. 2001; 29:188–192.
9. Wang Y, Wang VM, Chan CC. The role of anti-inflammatory agents in age-related macular degeneration (AMD) treatment. Eye. 2011; 25:127–139. [PubMed: 21183941]
10. Matsuda S, Gomi F, Oshima Y, Tohyama M, Tano Y. Vascular endothelial growth factor reduced and connective tissue growth factor induced by triamcinolone in ARPE19 cells under oxidative stress. Invest. Ophthalmol. Vis. Sci. 2005; 46:1062–1068. [PubMed: 15728566]
11. Elman MJ, Aiello LP, Beck RW, Bressler NM, Bressler SB, Edwards AR, et al. Randomized trial evaluating ranibizumab plus prompt or deferred laser or triamcinolone plus prompt laser for diabetic macular edema. Ophthalmology. 2010; 117:1064–77. e35. [PubMed: 20427088]
12. Gopal, Lekha; Sharma, Tarun. Use of intravitreal injection of triamcinolone acetonide in the treatment of age-related macular degeneration. Ind. J. Ophthalmol. 2007; 55(6):431.
13. Yeung CK, Chan KP, Chiang SWY, Pang CP, Lam DSC. The toxic and stress responses of cultured human retinal pigment epithelium (ARPE19) and human glial cells (SVG) in the presence of triamcinolone. Invest. Ophthalmol. Vis. Sci. 2003; 44:5293–5300. [PubMed: 14638729]
14. Durairaj C, Kadam RS, Chandler JW, Hutcherson SL, Kompella UB. Nanosized dendritic polyguanidilyated translocators for enhanced solubility, permeability, and delivery of gatifloxacin. Invest. Ophthalmol. Vis. Sci. 2010; 51:5804–5816. [PubMed: 20484584]
15. Holden CA, Tyagi P, Thakur A, Kadam R, Jadhav G, Kompella UB, et al. Polyamidoamine dendrimer hydrogel for enhanced delivery of antiglaucoma drugs. Nanomed. Nanotechnol. Biol. Med. 2012; 8:776–783.
16. Chung H, Hwang JJ, Koh JY, Kim J-g, Yoon YH. Triamcinolone acetonide-mediated oxidative injury in retinal cell culture: comparison with dexamethasone. Invest. Ophthalmol. Vis. Sci. 2007; 48:5742–5749. [PubMed: 18055827]
17. Narayanan R, Mungcal JK, Kenney MC, Seigel GM, Kuppermann BD. Toxicity of triamcinolone acetonide on retinal neurosensory and pigment epithelial cells. Invest. Ophthalmol. Vis. Sci. 2006; 47:722–728. [PubMed: 16431973]
18. Chang Y-S, Lin C-F, Wu C-L, Kuo P-Y, Wu F-S, Shieh C-C, et al. Mechanisms underlying benzyl alcohol cytotoxicity (triamcinolone acetonide preservative) in human retinal pigment epithelial cells. Invest. Ophthalmol. Vis. Sci. 2011; 52:4214–4222. [PubMed: 21345998]
19. Kleinman ME, Westhouse SJ, Ambati J, Pearson PA, Halperin LS. Triamcinolone crystal size. Ophthalmology. 2010; 117(1654):e1–e4. [PubMed: 20682380]
20. Kambhampati SP, Kannan RM. Dendrimer nanoparticles for ocular drug delivery. J. Ocul. Pharmacol. Ther. 2013; 29:151–165. [PubMed: 23410062]
21. Chaplot SP, Rupenthal ID. Dendrimers for gene delivery - a potential approach for ocular therapy. J Pharm. Pharmacol. 2014; 66:542–556. [PubMed: 24635556]
22. Sk UH, Kambhampati SP, Mishra MK, Lesniak WG, Zhang F, Kannan RM. Enhancing the efficacy of Ara-C through conjugation with PAMAM dendrimer and linear PEG: a comparative study. Biomacromolecules. 2013; 14:801–810. [PubMed: 23373724]

23. Mishra MK, Beaty CA, Lesniak WG, Kambhampati SP, Zhang F, Wilson MA, et al. Dendrimer brain uptake and targeted therapy for brain injury in a large animal model of hypothermic circulatory arrest. ACS Nano. 2014; 8:2134–2147. [PubMed: 24499315]
24. Vandamme TF, Brobeck L. Poly(amidoamine) dendrimers as ophthalmic vehicles for ocular delivery of pilocarpine nitrate and tropicamide. J. Control. Release. 2005; 102:23–38. [PubMed: 15653131]
25. Iezzi R, Guru BR, Glybina IV, Mishra MK, Kennedy A, Kannan RM. Dendrimer-based targeted intravitreal therapy for sustained attenuation of neuroinflammation in retinal degeneration. Biomaterials. 2012; 33:979–988. [PubMed: 22048009]
26. Lesniak WG, Mishra MK, Jyoti A, Balakrishnan B, Zhang F, Nance E, et al. Biodistribution of fluorescently labeled PAMAM dendrimers in neonatal rabbits: effect of neuroinflammation. Mol. Pharm. 2013; 10:4560–4571. [PubMed: 24116950]
27. Kannan S, Dai H, Navath RS, Balakrishnan B, Jyoti A, Janisse J, et al. Dendrimer-based postnatal therapy for neuroinflammation and cerebral palsy in a rabbit model. Sci. Transl. Med. 2012; 4:130ra46.
28. Mastorakos P, Kambhampati SP, Mishra MK, Wu T, Song E, Hanes J, et al. Hydroxyl PAMAM dendrimer-based gene vectors for transgene delivery to human retinal pigment epithelial cells. Nanoscale. 2014
29. Mansoor S, Kuppermann B, Kenney MC. Intraocular sustained-release delivery systems for triamcinolone acetonide. Pharm. Res. 2009; 26:770–784. [PubMed: 19184374]
30. Hong J, Kim B-K, Lim H, Lee S, Lee SJ. Identification and characterization of triamcinolone acetonide, a microglial-activation inhibitor. Immunopharmacol. Immunotoxicol. 2012; 34:912–918. [PubMed: 22551518]
31. Macky TA, Oelkers C, Rix U, Heredia ML, Künzel E, Wimberly M, et al. Synthesis, pharmacokinetics, efficacy, and rat retinal toxicity of a novel mitomycin C-triamcinolone acetonide conjugate. J. Med. Chem. 2002; 45:1122–1127. [PubMed: 11855992]
32. Valamanesh F, Berdugo M, Sennlaub F, Savoldelli M, Goumeaux C, Houssier M, et al. Effects of triamcinolone acetonide on vessels of the posterior segment of the eye. Mol. Vis. 2009; 15:2634–2648. [PubMed: 20011077]
33. Penfold PL, Wen L, Madigan MC, King NJC, Provis JM. Modulation of permeability and adhesion molecule expression by human choroidal endothelial cells. Invest. Ophthalmol. Vis. Sci. 2002; 43:3125–3130. [PubMed: 12202538]
34. Krieglstein CF, Granger DN. Adhesion molecules and their role in vascular disease. Am. J. Hypertens. 2001; 14:S44–S54.
35. Penfold PL, Wen L, Madigan MC, Gillies MC, King NJC, Provis JM. Triamcinolone acetonide modulates permeability and intercellular adhesion molecule-1 (ICAM-1) expression of the ECV304 cell line: implications for macular degeneration. Clin. Exp. Immunol. 2000; 121:458–465. [PubMed: 10971511]
36. Wang Y-S, Friedrichs U, Eichler W, Hoffmann S, Wiedemann P. Inhibitory effects of triamcinolone acetonide on bFGF-induced migration and tube formation in choroidal microvascular endothelial cells. Graefe's Arch. Clin. Exp. Ophthalmol. 2002; 240:42–48. [PubMed: 11954780]
37. Pereira AD, Santos MCM, Costa VM, Pianetti GR, Da Silva GA. Development and validation of a high performance liquid chromatographic method for determination of triamcinolone acetonide from polyurethane intraocular implants. Int. J. Pharm. Pharm. Sci. 2012; 4(4):132–136.
38. Bosnjakovic A, Mishra MK, Ren W, Kurtoglu YE, Shi T, Fan D, et al. Poly(amidoamine) dendrimer-erythromycin conjugates for drug delivery to macrophages involved in periprosthetic inflammation. Nanomed. Nanotechnol. Biol. Med. 2011; 7:284–294.
39. Gruneich JA, Price A, Zhu J, Diamond SL. Cationic corticosteroid for nonviral gene delivery. Gene Ther. 2004; 11:668–674. [PubMed: 14724671]
40. Ma K, Hu M-X, Qi Y, Zou J-H, Qiu L-Y, Jin Y, et al. PAMAM-triamcinolone acetonide conjugate as a nucleus-targeting gene carrier for enhanced transfer activity. Biomaterials. 2009; 30:6109–6118. [PubMed: 19656564]

41. Szurman P, Kaczmarek R, Spitzer MS, Jaissle GB, Decker P, Grisanti S, et al. Differential toxic effect of dissolved triamcinolone and its crystalline deposits on cultured human retinal pigment epithelium (ARPE19) cells. Exp. Eye Res. 2006; 83:584–592. [PubMed: 16684520]
42. Henn A, Lund S, Hedtjam M, Porzgen P, Leist M. The suitability of BV2 cells as alternative model system for primary microglia cultures or animal experiments of brain inflammation. Eur. J. Cell Biol. 2009; 88:72.
43. Wang B, Navath RS, Romero R, Kannan S, Kannan R. Anti-inflammatory and anti-oxidant activity of anionic dendrimer-N-acetyl cysteine conjugates in activated microglial cells. Int. J. Pharm. 2009; 377:159–168. [PubMed: 19463931]
44. Glybina IV, Kennedy A, Ashton P, Abrams GW, Iezzi R. Photoreceptor neuroprotection in RCS rats via low-dose intravitreal sustained-delivery of fluocinolone acetonide. Invest. Ophthalmol. Vis. Sci. 2009; 50:4847–4857. [PubMed: 19407016]
45. Paulo CS, Pires das Neves R, Ferreira LS. Nanoparticles for intracellular-targeted drug delivery. Nanotechnology. 2011; 22:494002. [PubMed: 22101232]
46. Carrillo-de Sauvage MA, Maatouk L, Arnoux I, Pasco M, Sanz Diez A, Delahaye M, et al. Potent and multiple regulatory actions of microglial glucocorticoid receptors during CNS inflammation. Cell Death Differ. 2013; 20:1546–1557. [PubMed: 24013726]
47. Zhang K, Zhang L, Weinreb RN. Ophthalmic drug discovery: novel targets and mechanisms for retinal diseases and glaucoma. Nat. Rev. Drug Discov. 2012; 11:541–559. [PubMed: 22699774]
48. Ma W, Zhao L, Fontainhas AM, Fariss RN, Wong WT. Microglia in the mouse retina alter the structure and function of retinal pigmented epithelial cells: a potential cellular interaction relevant to AMD. PLoS One. 2009; 4:e7945. [PubMed: 19936204]
49. Ambati J, Atkinson JP, Gelfand BD. Immunology of age-related macular degeneration. Nat. Rev. Immunol. 2013; 13:438–451. [PubMed: 23702979]
50. McCarthy CA, Widdop RE, Deliyanti D, Wilkinson-Berka JL. Brain and retinal microglia in health and disease: an unrecognized target of the renin-angiotensin system. Clin. Exp. Pharmacol. Physiol. 2013; 40:571–579. [PubMed: 23601050]
51. Blaauwgeers HGT, Holtkamp GM, Rutten H, Witmer AN, Koolwijk P, Partanen TA, et al. Polarized vascular endothelial growth factor secretion by human retinal pigment epithelium and localization of vascular endothelial growth factor receptors on the inner choriocapillaris: evidence for a trophic paracrine relation. Am. J. Pathol. 1999; 155:421–428. [PubMed: 10433935]
52. Felinski EA, Antonetti DA. Glucocorticoid regulation of endothelial cell tight junction gene expression: novel treatments for diabetic retinopathy. Curr. Eye Res. 2005; 30:949–957. [PubMed: 16282129]
53. Ebrahem Q, Minamoto A, Hoppe G, Anand-Apte B, Sears JE. Triamcinolone acetonide inhibits IL-6- and VEGF-induced angiogenesis downstream of the IL-6 and VEGF receptors. Invest. Ophthalmol. Vis. Sci. 2006; 47:4935–4941. [PubMed: 17065510]
54. Nauck M, Karakiulakis G, Perruchoud AP, Papakonstantinou E, Roth M. Corticosteroids inhibit the expression of the vascular endothelial growth factor gene in human vascular smooth muscle cells. Eur. J. Pharmacol. 1998; 341:309–315. [PubMed: 9543253]
55. Benson WB. A randomized trial comparing the efficacy and safety of intravitreal triamcinolone with standard care to treat vision loss associated with macular edema secondary to branch retinal vein occlusion. Evidence-Based Ophthalmol. 2010; 11:22–23. http://dx.doi.org/10.1097/IEB.0b013e3181c70dc3.

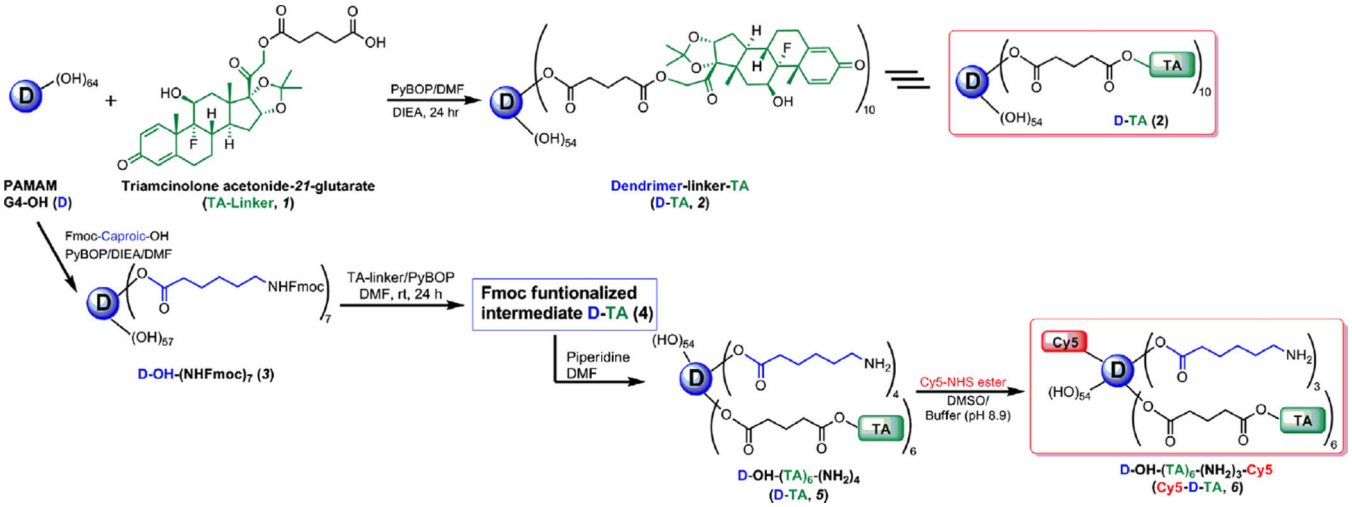

Fig. 1. Preparation of the dendrimer conjugates

Preparation of the dendrimer-triamcinolone acetonide conjugate (D-TA, ***2***); and Cy5-labeled dendrimer-TA conjugate (Cy5-D-TA, ***6***). (For interpretation of the references to color in this figure legend, the reader is referred to the web version of this article.)

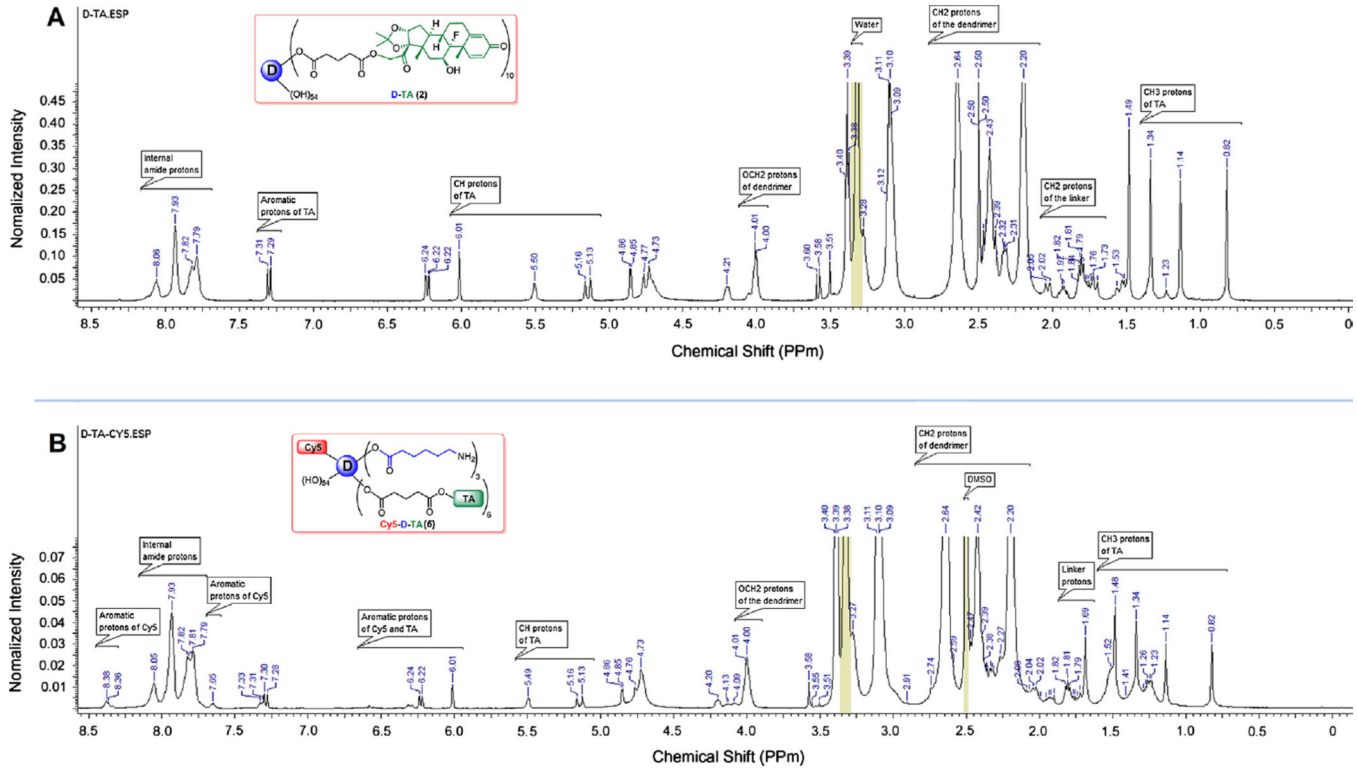

Fig. 2.

Proton NMR spectra of (**A**) dendrimer-triamcinolone acetonide conjugate (D-TA, ***2***) and (**B**) Cy5-labeled dendrimer-TA conjugates (Cy5-D-TA, **6**) in DMSO-d_6. (For interpretation of the references to color in this figure legend, the reader is referred to the web version of this article.)

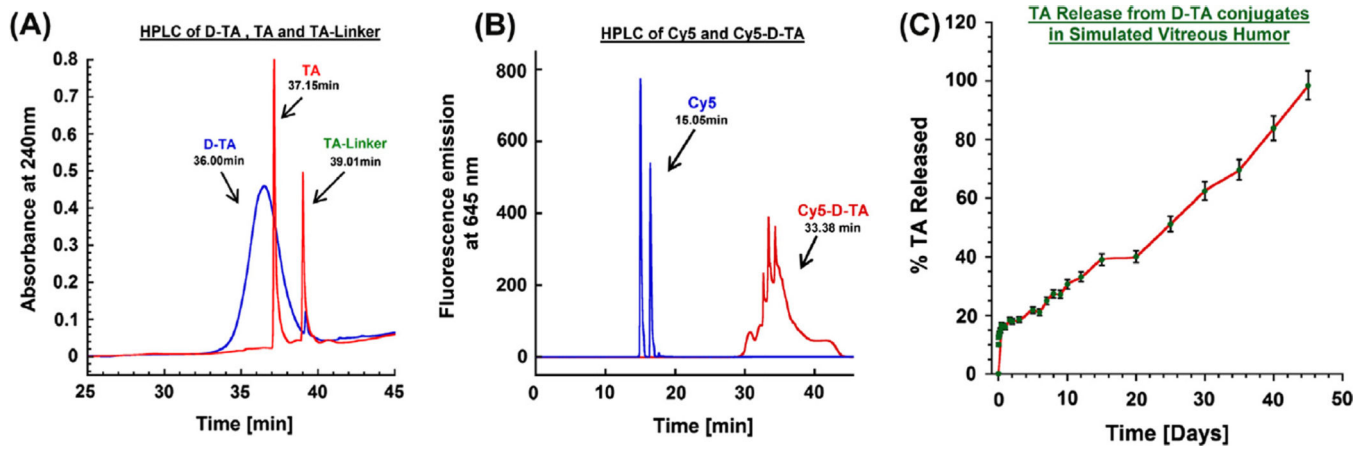

Fig. 3. Characterization of prepared conjugates

(A) HPLC chromatograms of D-TA (36.00 min), TA and TA-Linker both spiked together at equal weight basis (37.15 and 39.01 min respectively) monitored at 240 nm. (**B**) HPLC chromatogram of Cy5-D-TA (33.38 min) and free Cy5 (15.05 min) monitored at 645 nm fluorescence emission. **(C)** Drug release profile from D-TA conjugates in simulated vitreous humor. (For interpretation of the references to color in this figure legend, the reader is referred to the web version of this article.)

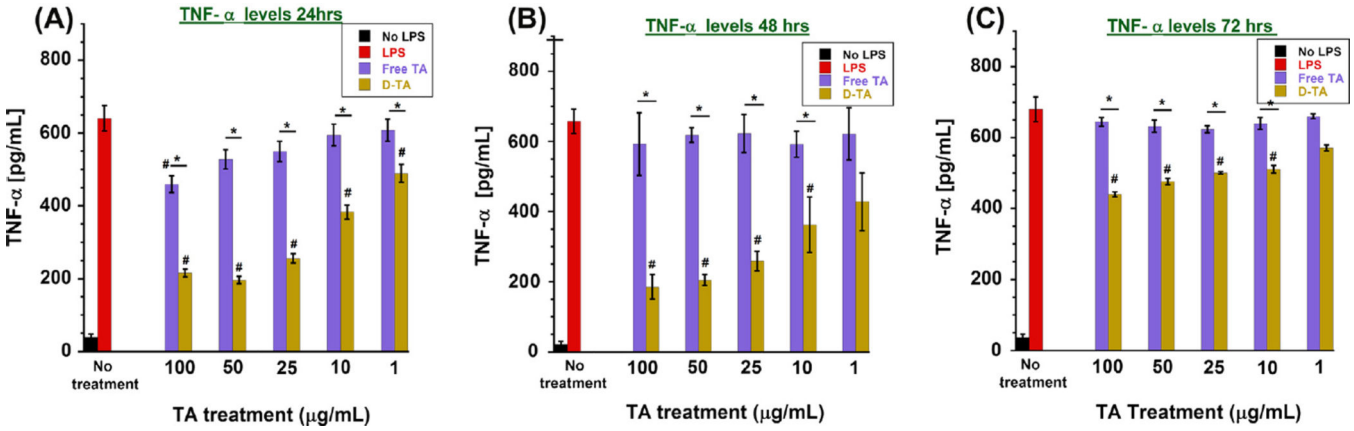

Fig. 4. Anti-inflammatory activity of D-TA (TNF-α release ELISA): Murine microglial cells (BV-2)

(passage 18) were activated using LPS (100 ng/mL) and treated with indicated concentrations of free TA and D-TA containing equivalent amount that of free TA for 12 h and replaced with LPS medium. Five samples (medium supernatant) were used for each group at indicated time point post treatment, TNF-α was measured using mouse TNF-α ELISA Kit, **(A)** 24 h D-TA treatment, **(B)** 48 h post D-TA treatment and **(C)** 72 h post D-TA indicating TNF-α suppression data represents mean ± SEM $^{*}P < 0.01$ vs free TA and $^{\#}P < 0.01$ vs group of LPS. (For interpretation of the references to color in this figure legend, the reader is referred to the web version of this article.)

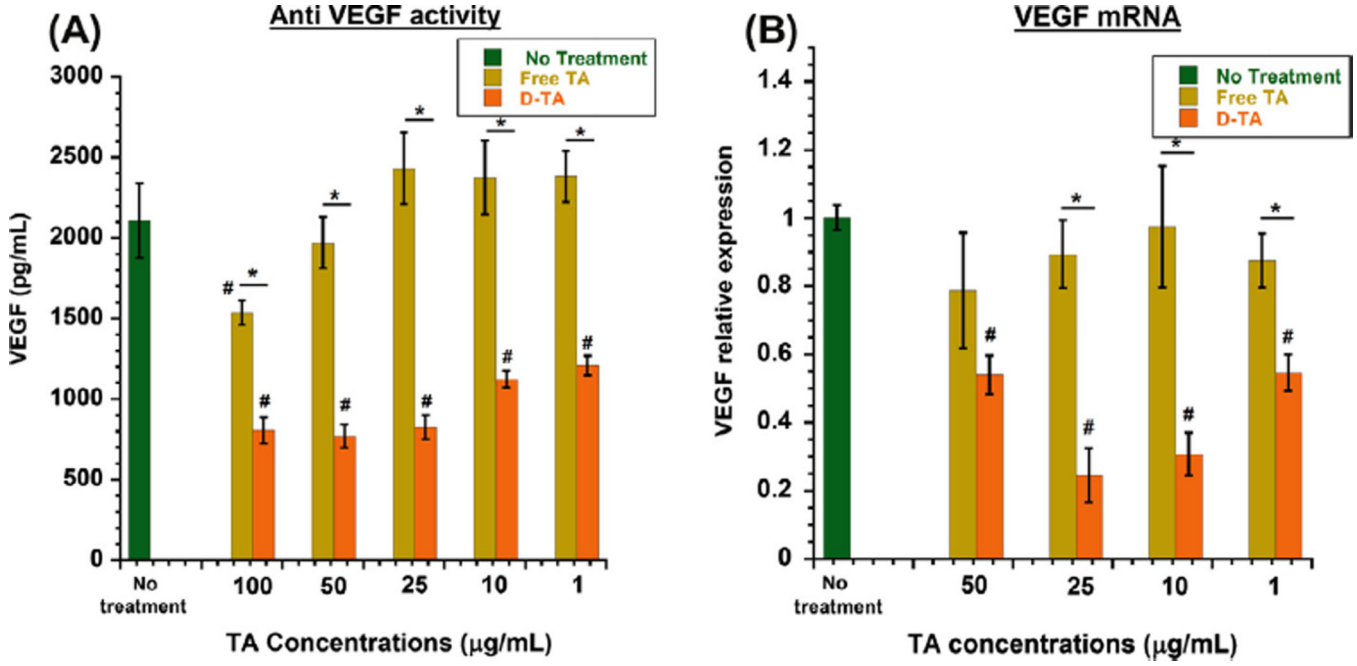

Fig. 5. Anti-VEGF activity of D-TA in human retinal pigment epithelial cells

ARPE-19 (passage 21) were subjected to hypoxia for 6 h and treated with D-TA and free TA (equivalent drug basis) at indicated concentrations for 24 h and replaced with culture medium. 24 h post treatment VEGF was analyzed using human VEGF ELISA kit and RT-PCR for mRNA expression **(A)** VEGF secretion analysis in culture medium using ELISA ($n = 6$) and **(B)** VEGF mRNA expression levels relative to GAPDH using RT-PCR ($n = 3$) data denote mean ± SEM, $^{*}P < 0.01$ vs free TA and $^{\#}P < 0.01$ vs group with no treatment. (For interpretation of the references to color in this figure legend, the reader is referred to the web version of this article.)

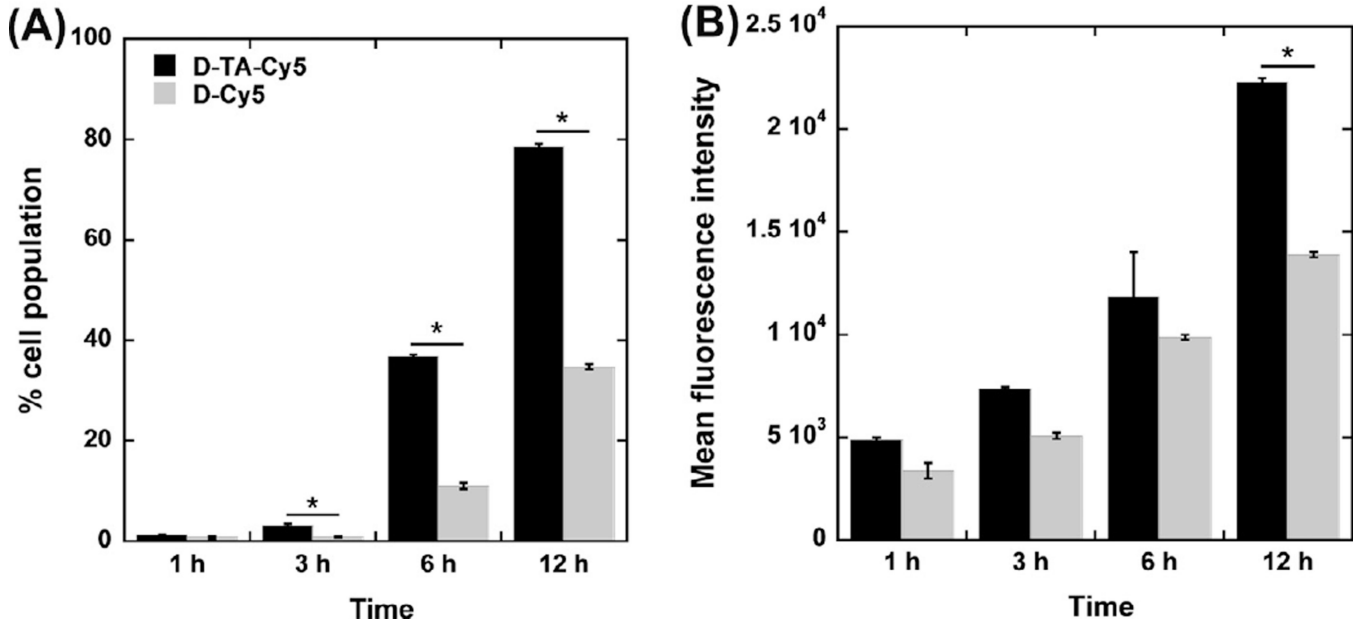

Fig. 6. Flow cytometric analysis of Cy5-D-TA and D-Cy5 cellular uptake by human retinal pigment epithelial ells (ARPE-19)

Cells were treated with Cy5-D-TA or D-Cy5 for 1 h, 3 h, 6 h and 8 h in order to assess the effect of TA-conjugation on dendrimer cell uptake. **(A)** The percentage of cell uptake at different time points demonstrated significantly higher uptake of Cy5-D-TA compared to D-Cy5 at 3 h, 6 h and 12 h of incubation. **(B)** The MFI of the cell population, indicating the absolute amount of dendrimer uptake, was higher following incubation with Cy5-D-TA compared to D-Cy5. Significance was only found at 12 h of incubation. $*P < 0.05$.

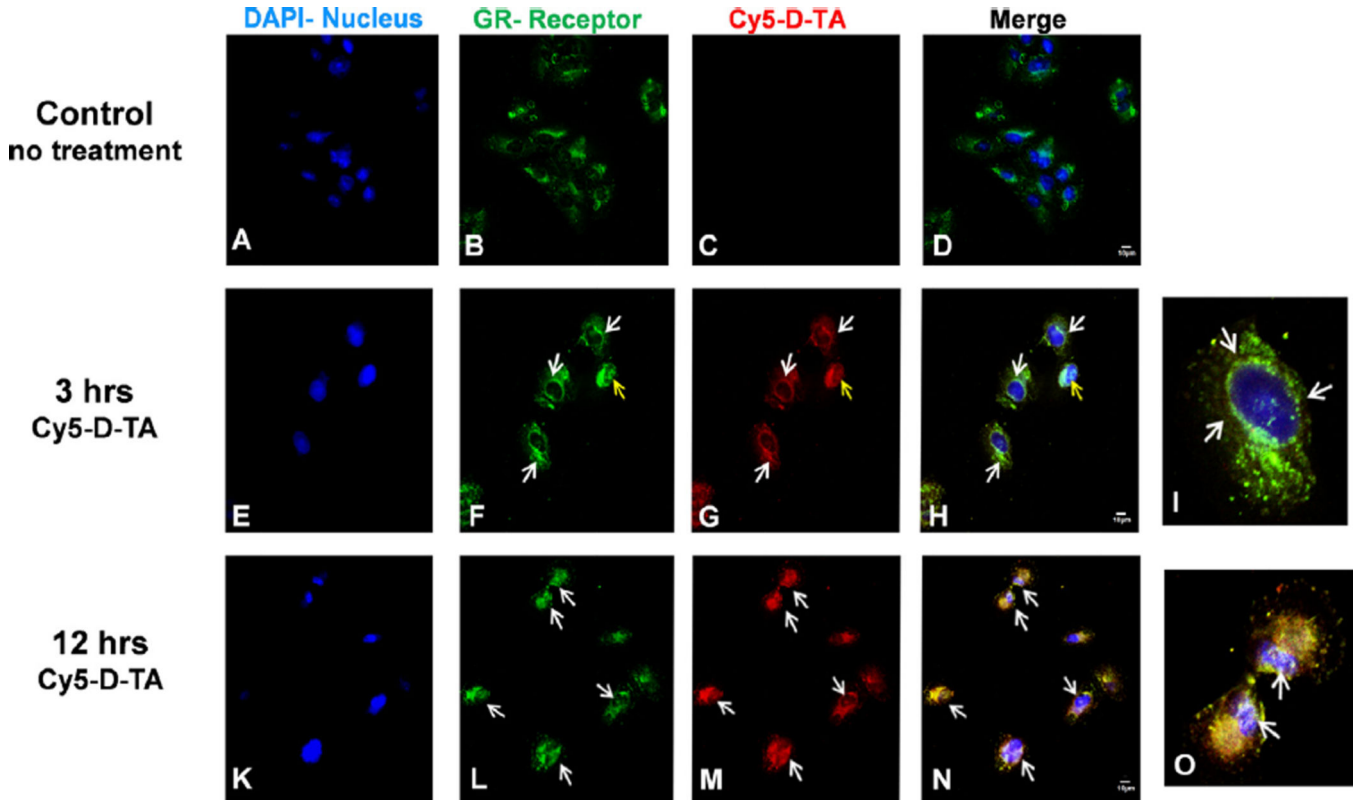

Fig. 7. Cellular uptake and nuclear localization of D-TA conjugates in ARPE-19 cells using confocal imaging

Cy5 labeled D-TA (Cy5-D-TA, red) was used to probe the intracellular localization of D-TA and it's binding to glucocorticoid receptor (GR, green) and nucleus (DAPI, blue). (**A–D**) control cells where GR receptors are in cytoplasm, (**E–H**) 3 h post Cy5-D-TA incubation white arrows indicating GR concentrated around the nucleus (I, digital zoom of single cell), (**K–N**) 12 h post D-TA-Cy5 incubation white arrows indicating nuclear localization of GR along with Cy5-D-TA (yellow merge) (**O**, digital zoom of single cell white arrows indicating the nuclear localization). The cells were imaged at 63× magnification, scale bar −10 μm. (For interpretation of the references to color in this figure legend, the reader is referred to the web version of this article.)